RESEARCH PAPER

Investigation of Corrosion Protection Properties of TiO_2-CdO Nanocomposite Coating Prepared by Sol-Gel Method on Copper

Farnaz Hajiyan pour, Mohsen Behpour, Mehdi Shabani-Nooshabadi*, Yaser Jafari

Department of Analytical Chemistry, Faculty of Chemistry, University Of Kashan, I.R. Iran

ARTICLE INFO

ABSTRACT

Sol–gel nanocomposite coatings have been investigated for copper metal as a potential replacement for the hazardous and banned hexavalent chromate conversion coatings. TiO_2–CdO nanocomposite thin films were deposited on copper using the sol–gel method. The sol-gel coatings were prepared using a sol obtained by the hydrolysis and condensation of tetra-o-butyl titanate. They were doped with cadmium oxide inhibitor to provide active corrosion protection. The synthesized coatings were characterized by X-ray diffraction (XRD) and atomic force microscopy (AFM). The anticorrosion performances of TiO_2-CdO nanocomposite coatings were investigated in 3.5% NaCl solution by the potentiodynamic polarization technique Tafle and electrochemical impedance spectroscopy (EIS). The potential corrosion increases from -210 mV versus Ag/AgCl (3M) for uncoated copper to -202 mV versus Ag/AgCl (3M) for TiO_2-CdO nanocomposite-coated copper electrodes. The results of this study clearly ascertain that the TiO_2-CdO nanocomposite has outstanding potential to protect the copper against corrosion in a chloride environment.

How to cite this article

INTRODUCTION

products; it results in the degradation and eventual failure of components and systems both in the processing and manufacturing industries and in the service life of many components. Corrosion control of metals and alloys is an expensive process and industries spend huge amounts to control this problem. It is estimated that the cost of corrosion in the developed countries such as the U.S. and European Union is about 3–5% of their gross national product [1].

The annual costs related to corrosion and corrosion prevention has been estimated to combine a significant part of the gross national product in the Western world. Although the value of such numbers is always debatable, corrosion issues are clearly is important in modern societies. In addition to the economic costs and technological delays, corrosion can lead to structural failures that have dramatic consequences for humans and the surrounding environment

Many papers are published each year about corrosion and corrosion protection of different metals. Among the metals investigated, the most important research about corrosion protection concentrates on copper, since copper is the basis of modern industry. Copper has been one of the preferred materials in industry due to its high electrical and thermal conductivities, mechanical workability, and its relatively noble properties. It is widely used in many applications in electronic industries and communications as a conductor in electrical power lines, and pipelines for domestic and industrial water utilities, including sea water, heat conductors, heat exchangers, etc. Thus, corrosion of copper and its inhibition in a variety of media, particularly when they contain chloride ions, have attracted the attention of a number of investigators [2].

* Corresponding Author Email: *m.shabani@kashanu.ac.ir*

Reports on the corrosion failures of bridges, buildings, aircrafts, automobiles, and gas pipelines are not unusual[3].

Corrosion poses a serious economic and industrial threat, as well as potential danger to humans. One of the current industrial practices for corrosion protection is to treat the surface of metals with chromium-containing compounds. However, chromium-containing coatings will be eventually banned1,2 because of its adverse health and environmental effects[4].

One of the most effective corrosion control techniques is the electrical isolation of the anode from the cathode [5, 6]. Sol gel technology is widely used for the preparation of inorganic materials from solutions containing inorganic or metal organic precursors, which are hydrolyzed to form inorganic polymers and colloids[7, 8]. Films can be deposited by spin coating, dip coating or electrophoresis, with the process repeated to build up coatings of thicknesses of up to tens of micrometers. Disadvantages of the sol gel deposition process are that the sol morphology needs to be carefully controlled to make sure continuous films and substrate wetting and that the films require drying and identifying. This may lead to film shrinkage and change of the underlying substrate due to the pH of the sol and the identifying thermal treatments. The application of ZrO_2 [9-11], Al_2O_3 [12], TiO_2-SiO_2 [13], CeO_2[11] and CeO_2-TiO_2 [14].

The obtained data also suggested that the organic-inorganic hybrid gel formulation might be tuned to contain nonsoluble chromium inhibitors regulating their effective concentrations within the coating layer[15]. The quick evolution of this specific research area and the potential contribution of sol–gel coatings as a corrosion inhibition system for metal substrates has led to several review publications[7]. As alternatives to the use chromate for corrosion protection of aluminum aerospace alloys[16], the use of sol-gel-derived coatings for improved corrosion resistance of aluminum and steel metal surfaces[17, 18] and magnesium alloys [19] had also been debated.

The novelty of the work involved is (1) the synthesis of TiO_2-CdO nanocomposites by sol-gel method instead of electrochemical synthesis, (2) synthesis TiO_2-CdO nanocomposites coatings on the surface of copper, most of which are synthesized on the surface of mild steel, (3) Use of TiO_2-CdO nanocomposites instead of TiO_2-CeO_2 and TiO2-SiO_2 nanocomposites, and (4) the aim of this study

is to investigate the inhibition effect corrosion of the TiO_2-CdO nanocomposite coatings synthesized by sol-gel method on copper in 3.5% NaCl solution by Tafel polarization, electrochemical impedance spectroscopy and the temperature effect method.

MATERIALS AND METHODS
Sample preparation
Titania and cadmium oxide sols were prepared using tetra-o-butyl titanate as precursor, ethanol as solvent, 37% hydrochloric acid, ethyl acetoacetate and distilled water, all from Merck Company.

TiO_2-CdO sols were prepared using tetra-o-butyl titanate according to the following procedure: 10 ml ethanol and 2.5 ml ethyl acetoacetate were mixed at room temperature. Then 2.5 ml tetra-o-butyl titanate and different concentrations of cadmium salts (0.15, 0.30, 0.45, 0.60 and 0.75 gr) were added the solution was stirred continuously for 2 h. In order to make sure enough degree of hydrolysis and to acquire homogeneity in the sol, 2 ml distilled water was carefully added to the solution within 30 min and kept stirring for a sufficient time. According to the composition of the nanocomposite, an appropriate amount of hydrochloric acid was added to the sol to reach the required pH for a stable sol.

The copper was used with purity of ≥99.9 wt% in the present study. The metal sheet was cut into rectangular samples of 1 cm × 1 cm ×0.1 cm soldered with Cu-wire for an electrical connection and mounted onto the epoxy resin to offer only one active flat surface exposed to the corrosive environment. Before each experiment the working electrode was abraded with a sequence of emery papers of different grades (320- 2000 grain size) and then electrode substrates were washed with distilled water, thoroughly degreased with ethanol and washed with distilled water. After natural drying in air flow, samples were heated in an oven at 120 °C for 15 min. The samples were then heat-treated at 300 °C for 60 min to enable oxide conversion and to remove the solvent and residual organics.

Characterization
For the purpose of X-ray diffraction (XRD) test, powder samples were prepared by drying the final sols in an oven at 120 °C for 1 h. XRD patterns were obtained using JEOL JDX-8030 diffraction system with Cu K α radiation (λ=1.5406 A°).The morphology of the sol-gel synthesized TiO_2-CdO nanocomposite coatings on copper was analyzed
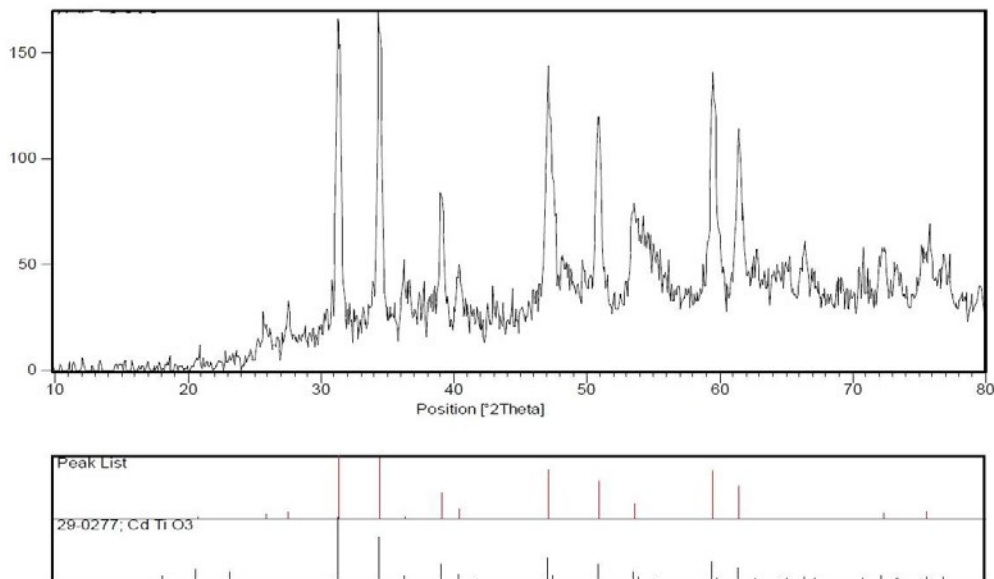
Fig. 1. XRD patterns of powder samples having TiO$_2$-CdO (0.75gr) nanocomposition

using a SERON model AIS-2100 scanning electron microscope (SEM) instrument operating at 10 kV. Surface morphology of the coatings was examined using Atomic force microscopy (AFM, Nanoscope V Tuna D3100).

Electrochemical experiments were carried out using a standard electrochemical three-electrode cell. Copper metal acts as working electrode (WE), silver–silver chloride (Ag/AgCl) as reference electrode and platinum was used as counter electrode. Polarization and impedance measurements were carried out using an AUTOLAB model PGSTAT30. The open circuit potential (OCP) was obtained by immersing the working electrode in the test solution 3.5% NaCl for 60min. Electrochemical impedance spectroscopy (EIS) measurements were carried out at corrosion potentials (OCP) across the frequency range 100 kHz-10 mHz, with a 10 mV amplitude of waveform. For potentiodynamic polarization measurements, potential was scanned in the range -200 to +200 mV at a scan rate 0.01 mV s^{-1}. All data for electrochemical measurements were analyzed using the NOVA 1.6 software.

RESULTS AND DISCUSSION
X-ray diffraction
Fig. 1 shows XRD patterns of powder samples having different constitution and heat treated at 120 °C for 1 h in air atmosphere. As it can be seen in this figure, the only phase that is formed in the sample having a composition of TiO$_2$–CdO is CdTiO$_3$ and, the TiO$_2$ content in TiO$_2$-CdO nanocomposition, anatase phase is formed in addition to the CdTiO$_3$ phase[20].

3.2. Scanning electron microscopy (SEM) analysis
Fig. 2 shows SEM micrographs of the TiO$_2$-CdO nanocomposite coatings on copper with 0.75 gr. Images show that nanoparticles are uniform, global and slightly agglomerated. Further observation indicates that the morphology of samples is very dense and uniform and may be beneficial to enhancing the corrosion protection due.

Electrochemical behavior studies
Electrochemical impedance spectroscopy (EIS)
Electrochemical process taking place at the open circuit potential was examined by electrochemical impedance spectroscopy. The impedance spectra for Nyquist plots were analyzed by fitting to the equivalent circuit model (Fig. 3).

EIS measurements (Fig. 4) of the copper electrode at its open-circuit potential after 60 min of immersion in 3.5% NaCl solution alone and in the presence of various concentrations of TiO$_2$-CdO nanocomposite coatings were performed over the frequency range from 100 kHz to 10 mHz. The diameter of Nyquist plots increased on increasing the concentration of TiO$_2$-CdO nanocomposite coatings indicating strengthening of inhibitive film.
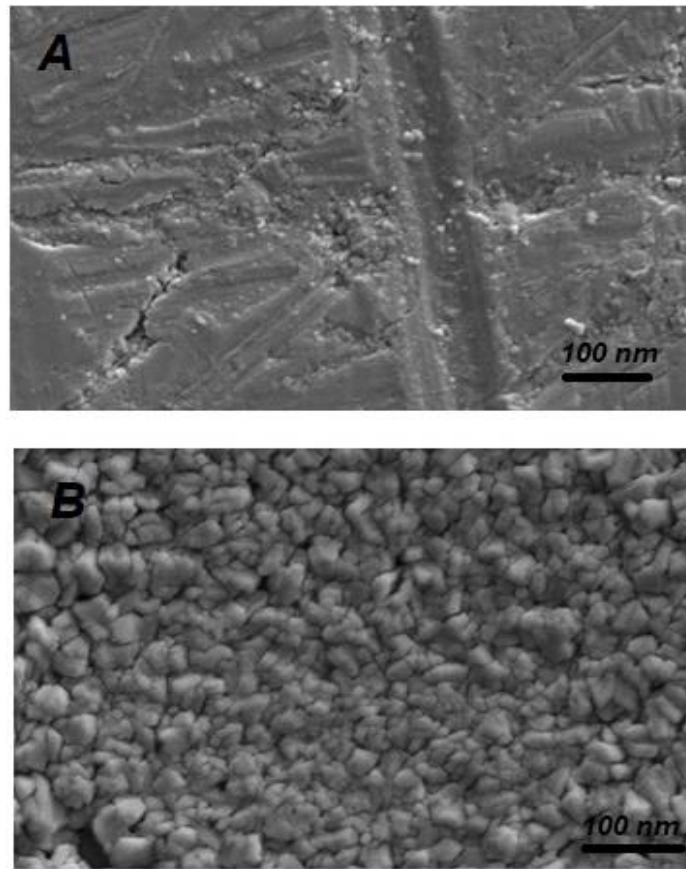
Fig. 2. SEM images of the (a) abraded copper and (b) sol-gel synthesized TiO$_2$-CdO nanocomposite coated copper with 0.75 gr CdO.
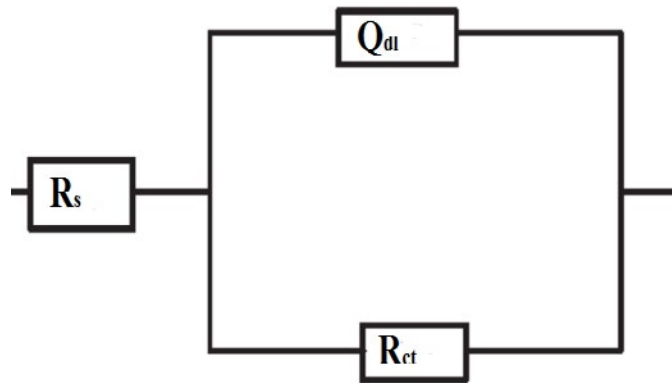
Fig. 3. Equivalent electrical circuit for the corrosion of copper in 3.5% NaCl solation.

The Nyquist plot contains a depressed semicircle with the center under the real axis, such behavior is characteristic for solid electrode which is attributed to surface roughness and inhomogeneities of metal electrodes. The existence of a single semicircle shows the presence of single charge transfer process during dissolution, which is unaffected by the presence of an TiO$_2$-CdO nanocomposite coatings[21].

The inhibition efficiency obtained from the charge-transfer resistance is calculated by the following relation [22]:

$$IE\left(\%\right)=\frac{R_{ct(c)}-R_{ct}}{R_{ct(c)}}\times100 \qquad (1)$$
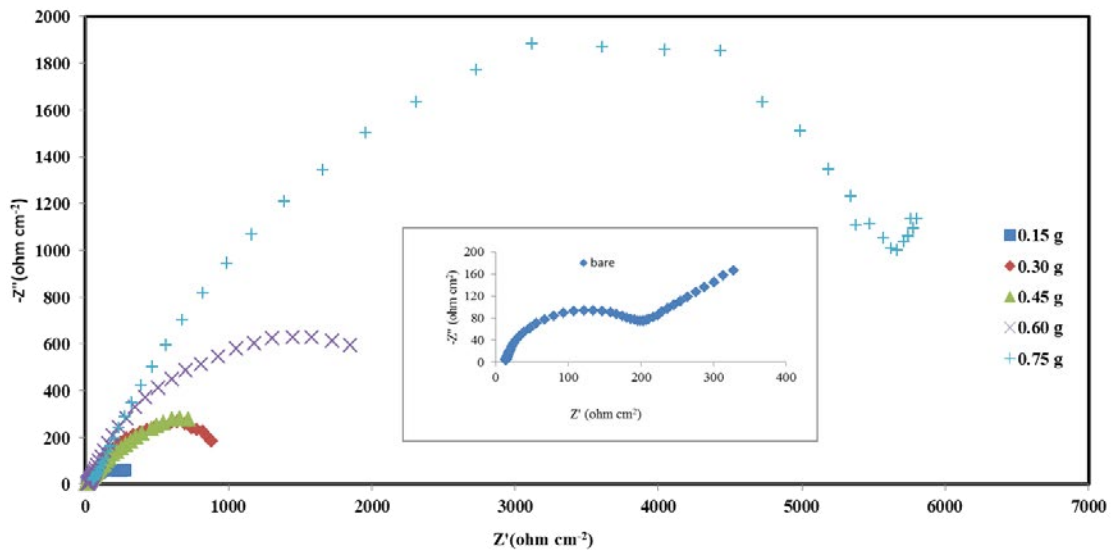
Fig. 4. Impedance spectra of copper in 3.5% NaCl solation with and without the nanocomposite coating.

Table1. Electrochemical impedance parameters for copper in 3.5% NaCl in absence and presence of TiO$_2$-CdO nanocomposite coating

TiO$_2$-CdO (g)	R$_s$ (Ω cm^2)	R$_{ct}$ (Ω cm^2)	n	Q Y$_0$ × 10^{-5} (μFcm^{-2})	IE$_{EIS}$ %
bare	15.32	154	0.78	10.41	-
0.15	16.91	405	0.41	4214	62.0
0.30	24.48	1176	0.51	1179	87.0
0.45	7.19	2322	0.39	2588	93.0
0.60	22.16	2586	0.57	852.9	94.0
0.75	50.00	6340	0.59	31.83	98.0

Where R$_{ct(c)}$ and R$_{ct}$ are the charge-transfer resistances in the presence and absence of the TiO$_2$-CdO nanocomposite coating.

As it can be seen from Fig. 4, the Nyquist plots contain depressed semicircles with the center under the real axis. Such behavior characteristic for solid electrodes and often referred to frequency dispersion could be attributed to different physical phenomena such as roughness and in homogeneity of the solid surfaces, impurities, grain boundaries and distribution of the surface-active sites [23]. Therefore, a constant phase element (CPE) instead of a capacitive element is used to get a more accurate fit of experimental data set. The impedance function of a CPE is defined by the mathematical expression given below [24] :

$$ZCPE = Q^{-1}(jw)^{-n} \qquad (2)$$

where Q is the CPE constant, v is the angular frequency, $j^2 = -1$ is the imaginary number and n is the CPE exponent which gives details about the degree of surface inhomogeneity resulting from surface roughness, inhibitor adsorption, porous layer formation, etc. The CPE, which is considered a surface irregularity of the electrode, causes a greater depression in Nyquist semicircle diagram [22], where the metal–solution interface acts as a capacitor with irregular surface. If the electrode surface is homogeneous and plane, the exponential value (n) becomes equal to 2 and the metal–solution interface acts as a capacitor with regular surface, i.e. The main parameters deduced from the analysis of Nyquist diagram for 3.5% NaCl solution containing various concentrations of TiO$_2$-CdO nanocomposite are given in Table 1. On increasing CdO concentration, the charge transfer resistance (R$_{ct}$) increased and capacitance (Y$_0$) decreased indicating that increasing CdO concentration decreased corrosion rate. This
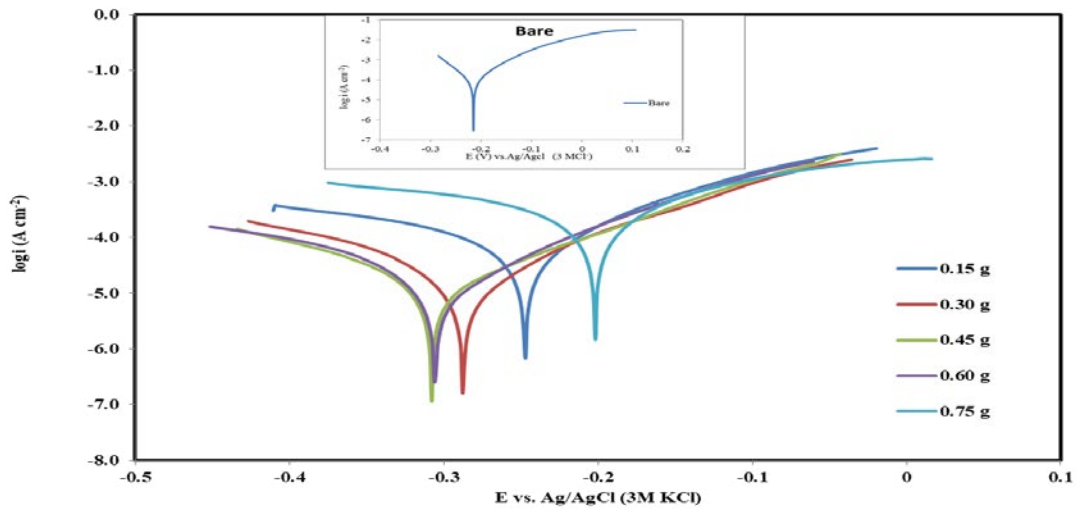
Fig. 5. Anodic and Cathodic polarization curves of copper in absence and present coatings in 3.5% NaCl media.

Table 2. Corrosion parameters of TiO$_2$-CdO nanocomposite coated on copper in 3.5% NaCl media.

TiO₂-CdO (g)	i_Corr (μA/cm²)	E_Corr (mV)	β_a (V/dec)	β_c (V/dec)	IE %
bare	330.28	-210	016.0	020.0	-
.150	640.12	-247	041.0	033.0	55.0
0.30	453.1	-288	015.0	019.0	95.0
0.45	101.1	-308	011.0	010.0	96.0
0.60	010.1	-306	033.0	050.0	96.4
0.75	.0011	-202	016.0	015.0	99.9

fact suggests that the inhibitor molecules acted by adsorption at the metal/solution interface [25].

Tafel polarization measurements

The effects of different concentration of TiO$_2$-CdO nanocomposite on the anodic and cathodic polarization curves in 3.5% NaCl solution are shown in Fig. 5.

Typical Tafel plots for the corrosion of copper in 3.5% NaCl solution and in the presence of TiO$_2$-CdO nanocomposite are shown in Fig. 5 where their electrochemical parameters are given in Table 2.

The displayed data clearly show that the corrosion current density (I$_{corr}$) values decreased in the presence of TiO$_2$-CdO nanocomposite indicating that the corrosion process of copper was suppressed in the presence of TiO$_2$-CdO nanocomposite. However, the lowest Icorr values were observed in the presence of highest CdO concentration. The percentage inhibition efficiency (IE %) for each TiO$_2$-CdO nanocomposite coating was calculated using the relationship given below and their values are mentioned in Table 2[26]:

$$IE\% = \frac{I_{corr} - I_{corr(c)}}{I_{corr}} \times 100 \qquad (3)$$

Where, I$_{corr}$ and I$_{corr(c)}$ are the corrosion current densities without and with the TiO$_2$-CdO nanocomposite, respectively.

From Table 2 it is evident that the highest inhibition efficiency was obtained for TiO$_2$-CdO nanocomposite (0.75 gr CdO) suggesting that this nanocomposite could serve as effective corrosion inhibitors. The values of IE% are in quite good agreement with the results obtained previously from EIS measurements.

As can be seen from Table 2, the corrosion potential for TiO$_2$-CdO nanocomposite coated copper has shifted to more positive potentials, about 200 mV vs. Ag/AgCl higher than the uncoated copper (anodic protection)[27].

Effect of temperature

Temperature has a great effect on the corrosion phenomenon. Generally, the corrosion current
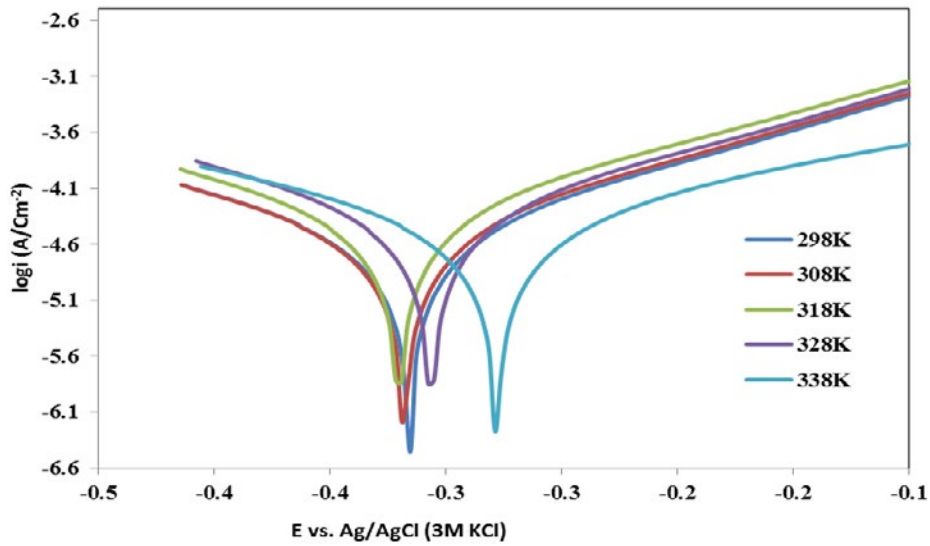
Fig. 6. The effect of temperature on the corrosion behavior of copper in the presence of coatings in temperature rang 298-338K.

Table3. Corrosion parameters of copper in 3.5% NaCl solution without nanocomposite coating in temperature rang 298-338K.

Temperature (K)	β$_c$ (mV/dec)	β$_a$ (mV/dec)	E$_{Corr}$ (mV)	i$_{Corr}$ (µA/cm^2)	IE %
298	20	16	-195	81.43	-
308	19	127	-183	76.43	-
318	12	172	-250	102.00	-
328	17	354	-322	104.20	-
338	22	18	-340	165.15	

Table 4. Corrosion parameters of copper in 3.5% NaCl solution with nanocomposite coating in temperature rang 298-338K.

Temperature (K)	β$_c$ (V/dec)	β$_a$ (V/dec)	E$_{Corr}$ (mV)	i$_{Corr}$ (µA/cm^2)	IE$_{EIS}$ %
298	38	37	-316	4.63	94
308	44	50	-318	6.14	92
318	75	82	-320	14.63	86
328	71	81	-306	14.93	85
338	37	39	-278	51.07	69

decreases with the rise of the temperature. For this purpose, we made polarization (Fig. 6) experiments in the range of temperature 298–338K, in the absence and presence of various concentrations of TiO$_2$-CdO nanocomposite coatings after 60 min of immersion. The corresponding data are shown in Table 3&4. From the Tables, it is clear that the IE(%) increases with the increase of concentration reaching a maximum value at a higher concentration (0.75 g CdO). This suggests that increase in the TiO$_2$-CdO nanocomposite coating concentration increases the number of

molecules adsorbed over the copper surface, blocking the active sites of acid attack and thereby protecting the metal from corrosion [28].

Ivanov[29] considers the increase of inhibition efficiency with temperature increases as the change in the nature of the adsorption mode. The inhibitor is being physically adsorbed at lower temperatures, while chemisorption is favored as temperature increases. Noor et al. [30] suggested increasing temperature, when chemical changes occur in the inhibitor molecules, leading to an increase in the electron density at the adsorption

Table 5. Activation parameters for the corrosion of copper in 3.5% NaCl solution with and without nanocomposite coating.

	ΔH$^*_{ads}$ (J mol^{-1})	E$_a$ (J mol^{-1})	ΔS$_{ads}^*$ (J mol^{-1} K^{-1})
bare	11.82	-14.40	-284.57
Nanocomposite	45.55	-48.01	-195.71

Table 6. Thermodynamic parameters for the adsorption of nanocomposite in 3.5% NaCl solution on the copper at 298K.

	Method	K$_{ads}$ (L g^{-1})	ΔG$°_{ads}$ (KJ mol^{-1})
Nanocomposite	Tafle	9.26	-22.62
	impedance	11.63	-23.19
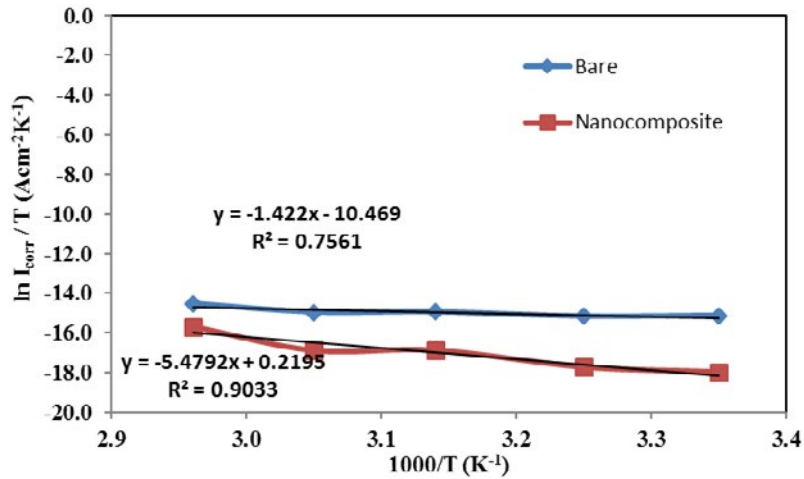
Fig. 7. Arrhenius plots for the corrosion of copper in 3.5% NaCl without and with nanocomposite coatings at different temperatures.

centers of the molecule, which causes an improvement in inhibition efficiency[31].

Thermodynamic activation parameters

In order to calculate the activation energy of the corrosion process and investigation of the mechanism of inhibition, gravimetric measurements were carried out at various temperatures (298–338 K) in the absence and presence of TiO$_2$-CdO nanocomposite coatings 3.5% NaCl. The results are given in Table 6. It was found that the rates of copper corrosion, in free and inhibited acid solutions increase with a rising of temperature. The dependence of the corrosion rate on temperature can be expressed by the Arrhenius equation[32].

The Arrhenius equation given below was used, to derive thermodynamic activation parameters without and with inhibitor[33]:

$$I_{corr} = K_{exp}\left(-Ea/RT\right) \quad (4)$$

Where R is the gas constant and K is the Arrhenius constant, E$_a$ is the activation energy, T the absolute temperature. Arrhenius plots of Ln I$_{corr}$ vs 1000/T for copper corrosion in 3.5% NaCl solution in the absence and presence of TiO$_2$-CdO nanocomposite coating are presented in Fig. 7.

The slope of Arrhenius plot is the apparent activation energy (E$_a$). The charge in enthalpy (ΔH) and entropy (ΔS) of activation was calculated by the transition-state equation given below[34]:

$$I_{corr} = RT/Nh \exp\left(\Delta S^*/R\right)\exp\left(-\Delta H^*/RT\right) \quad (5)$$

Where N is the Avogadro's number and h is the planck's constant. The plots of LnI$_{corr}$/T vs 1000/T are presented in Fig. 7 straight lines were obtained
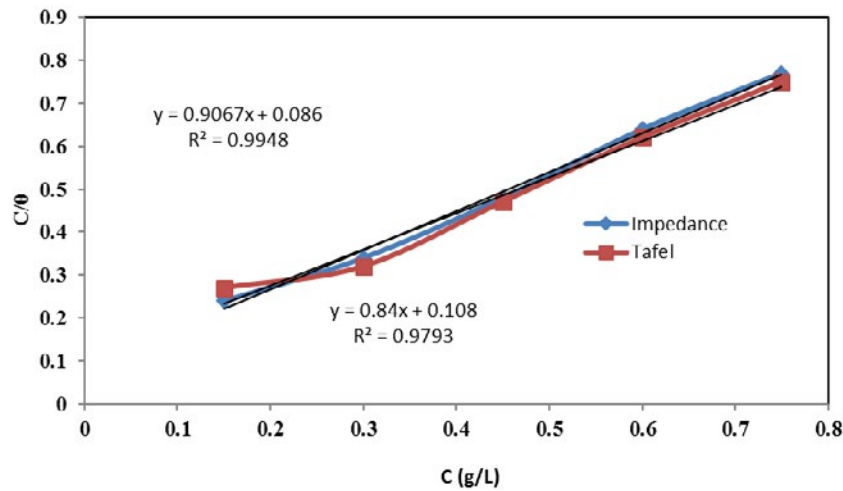
Fig. 8. Relationship between C/θ and inhibitor concentration with tofle and impedance methods.

with a slope of -ΔH, ΔS values were calculated from the intercepts of Ln I$_{corr}$/T axis and are given in Table 5 [28]. The value E$_a$ is found as -14.40, -48.01 for 3.5% NaCl solution and TiO$_2$-CdO nanocomposite coatings, respectively. Inspection of results shows that values of E$_a$ obtained in presence of TiO$_2$-CdO nanocomposite coatings are higher than inhibitor free solution.

The positive sign of the ΔH* reflects the endothermic nature of the copper dissolution process (Table 6). Large and negative values of ΔS* refer to that the activated complex in the rate determining step represents an association rather than a dissociation step, meaning that a decrease in disordering takes place on going from reactants to the activated complex[35].

Application of adsorption isotherm

From the polarization data, it is can be inferred that the essential step in the inhibition mechanism is the adsorption of the nanocomposite coating on the copper surface; therefore, the observed increase in corrosion inhibition efficiency results from improved adsorption of the TiO$_2$-CdO nanocomposite coating constituents on the copper surface. To describe the adsorption of TiO$_2$-CdO nanocomposite coating on the copper surface, several adsorption isotherms were tested, including Freundlich, Temkin, Frumkin, Bockris–Swinkels, Flory–Huggins and Langmuir isotherms. However, the best agreement was obtained using the Langmuir adsorption isothermal equation as follows[36]:

$$C/\Theta = 1/K_{ads} + C \qquad (6)$$

wre K$_{ads}$ is the adsorptive equilibrium constant, C is the concentration of the additives and Θ is surface coverage. Surface coverage (Θ, i.e. fractional inhibition efficiency) values for TiO$_2$-CdO nanocomposite coating as determined by the polarization measurements for various concentrations of the nanocomposite coating. As shown in Fig. 8 plotting of C vs. C/Θ results in a linear correlation. The strong correlation (R^2 > 0.99) suggests that the adsorption of the inhibitor on the copper surface obeyed this isotherm. Langmuir adsorption isotherm assumes that the adsorbed species occupy only one surface site and there are no interactions with other adsorbed species[37], features which closely describe the chemisorption process. It is necessary to mention here that, the Θ values obtained from the other employed techniques also obey the Langmuir adsorption isotherm[36].

The equilibrium constant for adsorption process is related to the free energy of adsorption ΔG$^0_{ads}$ is expressed by following equation [38]:

$$K_{ads} = \frac{1}{55.5} \exp(-\frac{\Delta G^0_{ads}}{RT}) \qquad (7)$$

Where R is the universal gas constant (8.314 J K^{-1} mol^{-1}), T is the thermodynamic temperature, 55.5 is the molar concentration of water in the solution expressed in 3.5% NaCl solution.

60
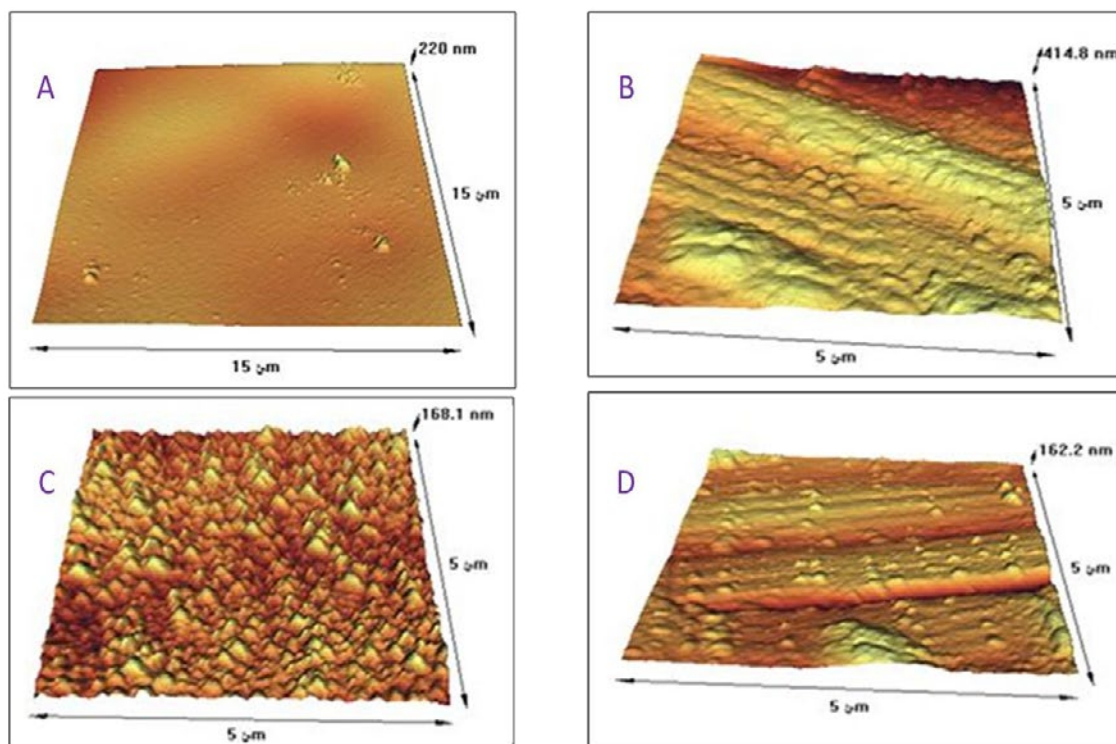
Fig. 9. AFM images of specimens: a) polished copper electrode b) pre-treated copper after corrosion c) TiO$_2$-CdO nanocomposite coated on copper d) TiO$_2$-CdO nanocomposite coated on copper in corrosion media.

The energy of adsorption could not have been calculated due to the unknown molecular mass of the TiO$_2$-CdO nanocomposite coating. The free energy of adsorption values, ΔG^0_{ads} were obtained for TiO$_2$-CdO nanocomposite coating and results show that the values of ΔG^0_{ads} is -22.62 and -23.19 kJ mol-1 for TiO$_2$-CdO nanocomposite coating in 3.5% NaCl solution by Tafel and EIS method, respectively. The negative values ΔG^0_{ads} means that adsorption of TiO$_2$-CdO nanocomposite coating on copper surface is a spontaneous process and furthermore the negative values of ΔG^0_{ads} also shows the strong interaction of the inhibitor molecule onto the copper surface [38].

Surface analysis

AFM is powerful techniques to investigative the surface morphology and study the influence of inhibitors on the generation and the progress of the corrosion at the metal/solution interface. AFM images (Fig. 9) of the polished copper and copper after immersion for 60min in 3.5% NaCl solution in absence and presence of TiO$_2$-CdO nanocomposite coating. These images showed

that decrease surface roughness for copper immersed in chloride solution in presence TiO$_2$-CdO nanocomposite coatings.

In Fig. 9, (a) presents the bare copper surface after polishing (before exposure to corrosive environment); (b) copper immersed in 3.5% NaCl solution without coating; (c) copper coated by TiO2-CdO nanocomposite and (d) copper immersed in 3.5% NaCl solution with TiO$_2$-CdO (0.75gr) nanocomposite coatings. It could be observed from the Fig. 8b that the copper surface was damaged in the absence of the TiO$_2$-CdO nanocomposite coatings and the surface is rough and porous. On the other hand, Fig. 8d appears to be less scratched in the presence of TiO$_2$-CdO nanocomposite coatings compared with that of the surface immersed in corrosive medium alone and the damage of the metal surface has diminished in presence of the TiO$_2$-CdO nanocomposite coatings, which is attributed to the formation of a protective layer by the constituents of TiO$_2$-CdO nanocomposite coatings. This indicates that TiO$_2$-CdO nanocomposite coatings hinders the dissolution of copper and thereby reduces the rate of corrosion of copper in 3.5% NaCl solution.

CONCLUSIONS

Sol-gel nanocomposite coatings doped with CdO inhibitor were developed for corrosion protection of copper. The coatings were smooth, crack-free with good adhesion and pencil hardness and also excellent anti-corrosion properties.

The corrosion current was influenced by CdO concentration 0.75 gr in the coating. Under static polarization conditions, the corrosion current of the coatings increased with CdO concentration due to the reduced barrier property. However, a remarkable decrease in corrosion current was observed after prolonged immersion in NaCl solution, particularly for coatings with higher CdO content.

The TiO₂-CdO nanocomposite coatings act as an anodic inhibitor for copper in 3.5% NaCl solution. The inhibition efficiency increases with increasing concentration of CdO(0.75 gr) with the highest inhibition efficiency being 99%. The percentage inhibition efficiency values obtained from polarization measurements are comparable with those obtained from EIS measurements. The surface analysis via AFM techniques indicates that the active molecules from TiO₂-CdO nanocomposite coatings absolutely retard the corrosion on the specimen surfaces.

ACKNOWLEDGEMENT

CONFLICT OF INTEREST

The authors declare that there is no conflict of interests regarding the publication of this manuscript.

REFERENCES

1. Bennett LH. Economic effects of metallic corrosion in the United States: a report to the Congress: The Bureau; 1978.
2. Sherif EM, Park S-M. Inhibition of Copper Corrosion in 3.0% NaCl Solution by N-Phenyl-1,4-phenylenediamine. Journal of The Electrochemical Society. 2005;152(10):B428.
3. Sørensen PA, Kiil S, Dam-Johansen K, Weinell CE., J. Coat. Tech. Rese., 2009;6(2):135-76.
4. Xing C, Zhang Z, Yu L, Zhang L, Bowmaker GA. Electrochemical corrosion behavior of carbon steel coated by polyaniline copolymers micro/nanostructures. RSC Advances. 2014;4(62):32718.
5. Moon D, Bennett M, editors. The effects of reactive element oxide coatings on the oxidation behaviour of metals and alloys at high temperatures. Materials Science Forum; 1989: Trans Tech Publ.
6. Stern KH. Metallurgical and ceramic protective coatings: Springer Science & Business Media; 1996.
7. Guo KW. A Review of Magnesium/Magnesium Alloys Corrosion and its Protection~!2009-10-01~!2009-11-25~!2010-02-11~! Recent Patents on Corrosion Science. 2010;2(1):13-21.
8. Nelson RL, Ramsay JDF, Woodhead JL, Cairns JA, Crossley JAA. The coating of metals with ceramic oxides via colloidal intermediates. Thin Solid Films. 1981;81(4):329-37.
9. Izumi K, Murakami M, Deguchi T, Morita A, Tohge N, Minami T. ChemInform Abstract: Zirconia Coating on Stainless Steel Sheets from Organozirconium Compounds. ChemInform. 1989;20(49).
10. Atik M, Zarzycki J, R'Kha C. Protection of ferritic stainless steel against oxidation by zirconia coatings. Journal of Materials Science Letters. 1994;13(4):266-9.
11. de Lima Neto P, Atik M, Avaca LA, Aegerter MA. Sol-gel ZrO2 coatings for chemical protection of stainless steel. Journal of Sol-Gel Science and Technology. 1994;1(2):177-84.
12. Biswas R, Woodhead J, Bhattacharaya A. Corrosion studies of inorganic sol-gel alumina coatings on 316 stainless steel., J.mat. sci. lett., 1997;16(20):1628-33.
13. Atik M, De Lima Neto P, Aegerter MA, Avaca LA. Sol-gel TiO2-SiO2 films as protective coatings against corrosion of 316L stainless steel in H2SO4 solutions. Journal of Applied Electrochemistry. 1995;25(2):142-8.
14. Kishi H, Okino Y, Honda M, Iguchi Y, Imaeda M, Takahashi Y, et al. The Effect of MgO and Rare-Earth Oxide on Formation Behavior of Core-Shell Structure inBaTiO3. Japanese Journal of Applied Physics. 1997;36(Part 1, No. 9B):5954-7.
15. Figueira RB, Silva CJR, Pereira EV. Organic–inorganic hybrid sol–gel coatings for metal corrosion protection: a review of recent progress. Journal of Coatings Technology and Research. 2014;12(1):1-35.
16. Twite RL, Bierwagen GP. Review of alternatives to chromate for corrosion protection of aluminum aerospace alloys. Progress in Organic Coatings. 1998;33(2):91-100.
17. Metroke TL, Parkhill RL, Knobbe ET. Passivation of metal alloys using sol–gel-derived materials — a review. Progress in Organic Coatings. 2001;41(4):233-8.
18. van Ooij WJ, Zhu D, Stacy M, Seth A, Mugada T, Gandhi J, et al. Corrosion protection properties of organofunctional silanes — An overview. Tsinghua Science and Technology. 2005;10(6):639-64.
19. Gray JE, Luan B. Protective coatings on magnesium and its alloys — a critical review. Journal of Alloys and Compounds. 2002;336(1-2):88-113.
20. Cheraghi H, Shahmiri M, Sadeghian Z. Corrosion behavior of TiO2–NiO nanocomposite thin films on AISI 316L stainless steel prepared by sol–gel method. Thin Solid Films. 2012;522:289-96.
21. Satapathy AK, Gunasekaran G, Sahoo SC, Amit K, Rodrigues PV. Corrosion inhibition by Justicia gendarussa plant extract in hydrochloric acid solution. Corrosion Science. 2009;51(12):2848-56.
22. Cruz J, Pandiyan T, García-Ochoa E. A new inhibitor for mild carbon steel: Electrochemical and DFT studies. Journal of Electroanalytical Chemistry. 2005;583(1):8-16.
23. Behpour M, Ghoreishi SM, Mohammadi N, Soltani N, Salavati-Niasari M. Investigation of some Schiff base compounds containing disulfide bond as HCl corrosion inhibitors for mild steel. Corrosion Science. 2010;52(12):4046-57.

24. Behpour M, Ghoreishi SM, Gandomi-Niasar A, Soltani N, Salavati-Niasari M. The inhibition of mild steel corrosion in hydrochloric acid media by two Schiff base compounds. Journal of Materials Science. 2009;44(10):2444-53.

25. Ashassi-Sorkhabi H, Shaabani B, Seifzadeh D. Effect of some pyrimidinic Shciff bases on the corrosion of mild steel in hydrochloric acid solution. Electrochimica Acta. 2005;50(16-17):3446-52.

26. Shabani-Nooshabadi M, Ghandchi MS. Santolina chamaecyparissus extract as a natural source inhibitor for 304 stainless steel corrosion in 3.5% NaCl. Journal of Industrial and Engineering Chemistry. 2015;31:231-7.

27. Huilong W, Jiashen Z, Jing L. Inhibition of the corrosion of carbon steel in hydrochloric acid solution by bisquaternary ammonium salt. Anti-Corrosion Methods and Materials. 2002;49(2):127-32.

28. Soltani N, Tavakkoli N, Khayatkashani M, Jalali MR, Mosavizade A. Green approach to corrosion inhibition of 304 stainless steel in hydrochloric acid solution by the extract of Salvia officinalis leaves. Corrosion Science. 2012;62:122-35.

29. Ivanov E. Inhibitors of Corrosion of Metals in Acid Media, Metallurgy. Handbook in Accordance with the State Service of Standard Reference Data'Moscow. 1986:175.

30. Noor EA, Al-Moubaraki AH. Thermodynamic study of metal corrosion and inhibitor adsorption processes in mild steel/1-methyl-4[4′(-X)-styryl pyridinium iodides/hydrochloric acid systems. Materials Chemistry and Physics. 2008;110(1):145-54.

31. Shabani-Nooshabadi M, Hoseiny FS, Jafari Y. Green Approach to Corrosion Inhibition of Copper by the Extract of Calligonum comosum in Strong Acidic Medium. Metallurgical and Materials Transactions A. 2014;46(1):293-9.

32. Behpour M, Ghoreishi SM, Khayatkashani M, Soltani N. Green approach to corrosion inhibition of mild steel in two acidic solutions by the extract of Punica granatum peel and main constituents. Materials Chemistry and Physics. 2012;131(3):621-33.

33. Obot IB, Obi-Egbedi NO, Umoren SA. Antifungal drugs as corrosion inhibitors for aluminium in 0.1M HCl. Corrosion Science. 2009;51(8):1868-75.

34. Bouklah M, Benchat N, Hammouti B, Aouniti A, Kertit S. Thermodynamic characterisation of steel corrosion and inhibitor adsorption of pyridazine compounds in 0.5 M H2SO4. Materials Letters. 2006;60(15):1901-5.

35. Solmaz R, Kardaş G, Çulha M, Yazıcı B, Erbil M. Investigation of adsorption and inhibitive effect of 2-mercaptothiazoline on corrosion of mild steel in hydrochloric acid media. Electrochimica Acta. 2008;53(20):5941-52.

36. Soltani N, Tavakkoli N, Khayat Kashani M, Mosavizadeh A, Oguzie EE, Jalali MR. Silybum marianum extract as a natural source inhibitor for 304 stainless steel corrosion in 1.0 M HCl. Journal of Industrial and Engineering Chemistry. 2014;20(5):3217-27.

37. Ali SA, Saeed MT, Rahman SU. The isoxazolidines: a new class of corrosion inhibitors of mild steel in acidic medium. Corrosion Science. 2003;45(2):253-66.

38. Afonso FS, Neto MMM, Mendonça MH, Pimenta G, Proença L, Fonseca ITE. Copper corrosion in soil: influence of chloride contents, aeration and humidity. Journal of Solid State Electrochemistry. 2009;13(11):1757-65.